

## Adsorption of Acid Blue 113 using Nanocarbon Spheres and its Kinetic and Isotherm Studies

V. PRIYA<sup>1,\*</sup>, S.K. KRISHNA<sup>1</sup>, V. SIVAKUMAR<sup>2</sup> and P. SIVAKUMAR<sup>3</sup>

<sup>1</sup>Department of Chemistry, Chikkaiah Naicker College, Erode-638004, India

<sup>2</sup>Department of Chemistry, Sri Vasavi College, Erode-638316, India

<sup>3</sup>Department of Chemistry, Arignar Anna Govt Arts College, Namakkal-637002, India

\*Corresponding author: E-mail: priyavelusamy.m.sc@gmail.com

Received: 19 January 2019;

Accepted: 6 March 2019;

Published online: 28 June 2019;

AJC-19432

Nanocarbon spheres were prepared from the stems of *Alternanthera sessilis*. Their characterization studies were performed and the application of nanocarbon spheres for the adsorption of acid blue 113 from the aqueous solution was studied. Effect of pH of effluent, effect of initial acid blue 113 concentration and the effect of solution temperature were analyzed. Pseudo-first order model, pseudo-second order model, Elovich model, Intra-particle diffusion model, Langmuir model, Freundlich model and thermodynamic parameters were used to evaluate the percentage and the amount of acid blue 113 dye removed. The kinetics follows multi-order and Langmuir type of isotherm. The  $\Delta G$ ,  $\Delta H$  and  $\Delta S$  parameters which relate to sorption energy were also evaluated. The outcome of the study indicates that nanocarbon sphere is a potential material for the sorption of acid blue 113 with good efficiency.

**Keywords:** Acid blue 113, Nanocarbon, Adsorption, Kinetic, Isotherm.

### INTRODUCTION

Owing to the increase of population, the release of wastewater from various industries has reached an uncontrollable level and the world is also in a need of more water, mainly in the form of treated water for agriculture (70 %), industries (80 %) and domestic (22 %) areas. Large amounts of water containing massive amount of contaminants are released every year [1]. Among all the contaminants dyes are the major portion which were released from many resources such as dyeing, paper, plastics, printing, leather, production of dyestuffs, rubber, etc., present in the wastewater [2-4]. The dye effluents cause major effects on humans, mammals and aquatic toxicity. Therefore, the elimination of dye effluents from industrial wastes is very important before releasing them into pure water bodies [5,6]. Various techniques were followed over many years for the removal of contaminants from wastewater such as electro coagulation [7], membrane filtration [8], biosorption [9], ozonation [10], coagulation and flocculation [11], electrochemical precipitation [12], etc. But these methods have some drawbacks in the removal of dye effectively from wastewater.

Adsorption is one of the most important techniques which have good efficiency, low cost, ease of operation and less amount of residue. In this process, the dye molecules are removed easily due to the attractive nature of the adsorbent over the dye molecules. Various adsorbents were discovered from organic and inorganic wastes e.g. waste coir pith [13], rotten saw dust [14], fly ash [15], recycled alum sludge [16], fire wood [17], coconut shells [18], activated carbon [19,20], clay-polymer nano composites [21], starch-based nano composites [22], etc., Adsorbent with high surface area is required for the effective removal of dye molecules. For high surface area adsorbent, nano structured adsorbent is need to be prepared. In the present work, the nanocarbon adsorbent was synthesized from the stems of *Alternanthera sessilis* and its characterization studies were carried out. The nanocarbon adsorbent is used for the removal of acid blue 113 dye.

### EXPERIMENTAL

Analytical grade chemicals were purchased and used for all the process without any further purification. Double distilled water was used for the preparation of all the solutions. Waste

engine oil was used as precursor for the preparation of carbon ball.

**Preparation of nanocarbon spheres:** *Alternanthera sessilis* stems were air dried and cut into pieces of size 2 to 5 cm length. The dried pieces were burnt in the muffle furnace for 1 h at 750 °C under constant flow of nitrogen at 0.1 bar. Carbonization takes place in the muffle furnace. The carbonized stems were washed twice with pure water and then with alcohol and dried in air oven at 110 °C for 24 h [23]. The carbonized stems were soaked in the waste engine oil for 30 min and dried in air for 1 h. The oil-soaked carbonized stems were burnt on the stainless steel grill using LPG as fuel with air and the temperature inside the chamber was maintained between 420 to 470 °C. The stems will burn at its ignition temperature, and the soot formed during burning was carefully collected from the dome-shaped surface of stainless steel lid (316SS) kept on the top of the combustion chamber. Excess exhaust gas and the ash formed during the combustion were removed through exhaust holes and the discharge opening at the bottom, respectively. The carbon collected was washed twice with distilled water and then with alcohol once. Activation of nanocarbon spheres was done in the microwave oven at 600 W of power for 10 min. Using Zeiss Electron microscope at a maximum magnification of  $41.14 \times 10^3$  zooming, the SEM images of nanocarbon spheres was viewed.

**Batch adsorption studies:** Acid blue 113, an anionic acid dye was investigated by varying certain parameters like solution pH, initial acid blue 113 concentration, solution temperature, *etc.* The molecular weight of acid blue 113 is 681.649 g/mol with the molecular formula  $C_{32}H_{21}N_5O_6S_2Na_2$ , C.I No. 26360 with  $\lambda_{max}$  of 570 nm. Stock solution of 1000 mg/L was prepared by using particular amount of dye dissolved in distilled water. From the stock solution the diluted solutions were prepared. The batch mode adsorption studies were carried out by taking 100 mL of dye solution of particular concentration with 100 mg of nanocarbon spheres in 250 mL reagent bottle (Borosil-R glass bottles) with tight lid and REMI orbital shaker. To maintain the pH of solution 1 M HCl and 1 M NaOH solutions were used. After agitation, the contents were centrifuged at 5000 rpm. The final concentration of the dye is estimated by measuring the optical density of acid blue 113 at  $\lambda_{max}$  of 570 nm in UV-VIS spectrometer (Model: Elico-BL198). Duplicate experiment was also carried out simultaneously and the maximum deviation for both the experiments was found to be less than 4 %.

Percentage removal and amount of acid blue 113 dye were calculated using the following equations:

$$\text{Dye removal (\%)} = \frac{C_o - C_t}{C_o} \times 100 \quad (1)$$

Amount of acid blue 113 removed per unit quantity of nanocarbon spheres:

$$q_t \text{ (mg/g)} = (C_o - C_t) \frac{V}{W} \quad (2)$$

where,  $C_o$  is the initial concentration,  $C_t$  is the concentration at time 't', V is the volume of dye solution in mL and W is the weight of adsorbent in g.

**Kinetic analysis:** The actual controlling mechanisms were assessed from the kinetic studies [24,25]. The adsorption of

acid blue 113 by nanocarbon spheres was studied using the kinetic models like pseudo-first order, pseudo-second order and Elovich model. The adsorption mechanism of acid blue 113 on nanocarbon spheres was evaluated using intraparticle diffusion kinetic model. The fundamental isotherm models Langmuir and Freundlich isotherm models were used. Thermodynamic parameters  $\Delta G$ ,  $\Delta H$  and  $\Delta S$  were calculated using van't Hoff plot.

## RESULTS AND DISCUSSION

**SEM morphology:** The SEM images of pure carbon sample indicate the presence of clusters of carbon nanospheres of sizes ranging between 50 and 80 nm (Fig. 1). The pH and  $pH_{ZPC}$  of nanocarbon sphere was below 7.0, could may be due to the presence of acidic functionalities. The bulk density is very small and the surface area of nanocarbon sphere is 700.7  $m^2/g$ , which is comparable with that of commercial variants (Table-1) [26].

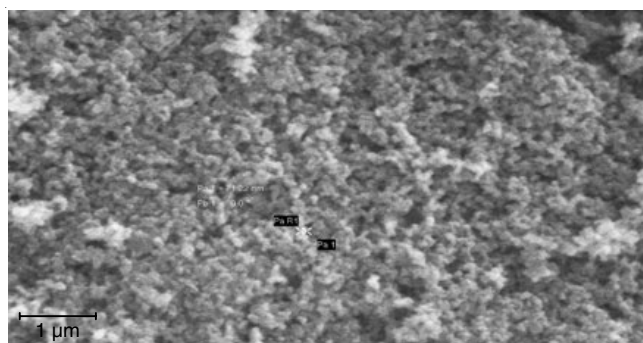


Fig. 1. SEM image of pure nanocarbon spheres

TABLE-1  
PROPERTIES OF NANOCARBON SPHERES

Properties	Nanocarbon spheres
pH	6.6
$pH_{ZPC}$	6.8
Bulk density (g/mL)	0.145
BET surface area ( $m^2/g$ )	700.7
Moisture content (%)	11.45
Volatile matter (%)	6.62

**Effect of pH on the adsorption of acid blue 113:** In any adsorption system, the pH is considered as one of the dominant parameters which has control over the adsorption of dye ion onto to the given adsorbent. Fig. 2 shows the variation of acid blue 113 adsorption onto nanocarbon spheres for an initial acid blue 113 concentration of 50 mg/L under different pH values ranged from 2.0 to 12.0.

At lower pH, the surface of nanocarbon spheres is protonated and the surface of nanocarbon spheres becomes positive, which attract the negatively charged dye anion. At lower pH, the electrostatic force of attraction between the nanocarbon sphere surface and acid blue 113 anion is more, which favours the adsorption of acid blue 113. On increasing the pH of the solution, the number of negative ions on the sorbent surface increases, which creates a repulsive force between the dye anion and the sorbent surface. When the pH is almost neutral, (pH around 7.0) the adsorption of acid blue 113 is purely due to diffusion through the micro- and meso-pores which are present

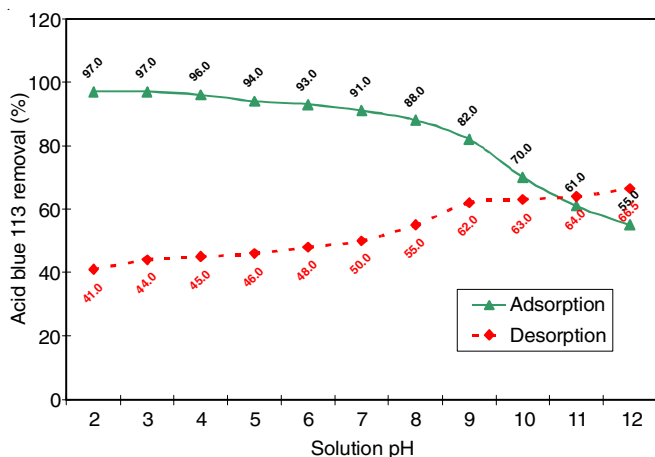


Fig. 2. Effect of pH on the adsorption and desorption of acid blue 113 dye

on the sorbent surface. If the pH of the solution exceeds the  $pH_{ZPC}$  of the sorbent, the sorbent surface becomes negative, which ultimately repels the negatively charged acid blue 113 anion and thereby acid blue 113 adsorption decreases drastically. At higher pH, electrostatic repulsion minimizes the dye adsorption on the surface as well as pore diffusion [27]. The adsorption of acid blue 113 is maximum at a pH of 2.0 and it decreases to 86.4% when the solution pH reaches 12.0. For large scale operations of acid blue 113 adsorption by nanocarbon spheres the solution must be adjusted to basic nature (*i.e.* pH of 10.0).

Desorption studies were performed to ascertain the reusability of nanocarbon sphere for many cycles during the adsorption of acid blue 113. A known quantity of acid blue 113 loaded nanocarbon sphere was shaken with distilled water until the equilibrium and the desorbed quantity of acid blue 113 was evaluated based on the optical density studies as stated in the adsorption studies. Fig. 2 showed that the desorption was minimum at a pH of 2.0 (41.0%) and it increases on increasing the pH from 2.0 to 12.0. At lower pH, the positively charged nanocarbon sphere will not favour desorption of acid blue 113, at higher pH, the negatively charged sorbent surface and the competitive  $OH^-$  ions will favour desorption. The adsorbent can be successfully employed up to 10 cycles with substantial amount of adsorption.

**Effect of initial dye concentration:** The effect of initial acid blue 113 concentration on its adsorption performance with nanocarbon sphere was evaluated by varying the concentration of the initial acid blue 113 from 25 to 100 mg/L for a fixed volume of 100 mL and an adsorbent dosage of 100 mg. The experimental kinetic data for the adsorption of acid blue 113 onto nanocarbon sphere by varying acid blue 113 concentration and the kinetic data at various temperatures were recorded.

From Fig. 3, it was clear that the rate of adsorption of acid blue 113 increases progressively with time and reaches equilibrium at 90 min. A great rate of adsorption was observed during the initial stage of adsorption. The rapid adsorption rate at the beginning is due to the high driving force from the solution side onto the bare nanocarbon sphere surface. At high initial acid blue 113 concentration, the concentration gradient between the solid liquid interfaces creates more driving force, which leads to high initial adsorption rate. The increase of acid blue 113 concentration does not have much influence on the

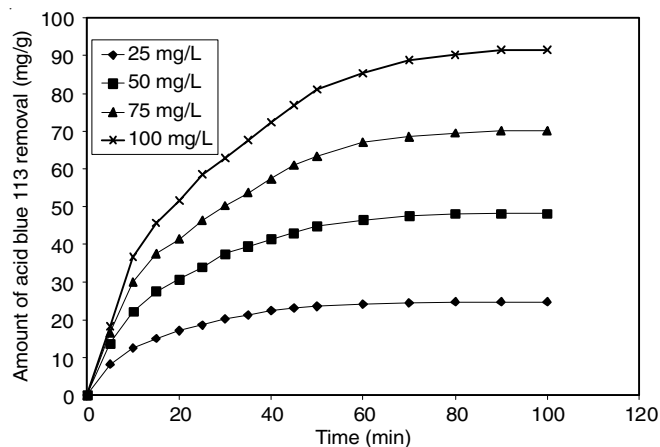


Fig. 3. Amount of acid blue 113 adsorption onto nanocarbon spheres - concentration variation

attainment of equilibrium. During the progression, the concentration gradient across the solid liquid interface diminishes and the speed of adsorption decreases.

The quantity of acid blue 113 adsorption by nanocarbon sphere increases from 24.72 to 91.60 mg/g on increasing the initial acid blue 113 concentration from 25 to 100 mg/L. The acid blue 113 removal percentage decreased from 98.86 to 91.60% with an increase of initial acid blue 113 concentration from 25 to 100 mg/L. The chance of surface sites accessibility for a given acid blue 113 dye molecule is more than at higher concentration. At higher initial concentrations, the number of sorbent sites per given number of dye molecule is less, which results in lower adsorption percentage.

**Effect of temperature:** During the chemisorption type of adsorption, the quantity of solute uptake increases with increases in temperature [25]. In case of physisorption, the rate of adsorption decreases with increase of temperature. The porous activated materials may have surface functionalities (which favour the chemisorption type of adsorption) and mesopores and micropores (which favour the physisorption type of adsorption). In some specific cases of adsorbent-adsorbate systems, both physisorption and chemisorption may operate simultaneously. In the present study, adsorption of acid blue 113 on to nanocarbon sphere increases from 48.17 to 49.51 mg/g on increasing the temperature from 30 to 45 °C for an initial nanocarbon sphere dye concentration of 50 mg/L. As observed from Fig. 4, an increase of adsorption with respect to temperature indicates the endothermic nature, which is favoured by raise in temperature [28]. Thermodynamical studies using van't Hoff plots is further essential for the conformation of endothermism involved for the acid blue 113 adsorption onto nanocarbon sphere.

**Kinetic analysis:** The adsorption of acid blue 113 by nanocarbon sphere was studied using the kinetic models like pseudo-first order, pseudo-second order and Elovich model. The adsorption mechanism of acid blue 113 on nanocarbon sphere was evaluated using intra-particle diffusion kinetic model [25].

**Pseudo-first order kinetic model:** The pseudo-first order plot for the adsorption of acid blue 113 onto nanocarbon sphere at various initial acid blue 113 concentration and temperatures are shown in Figs. 5 and 6, respectively. The results derived from the slope and intercept of linear plot are calculated. The

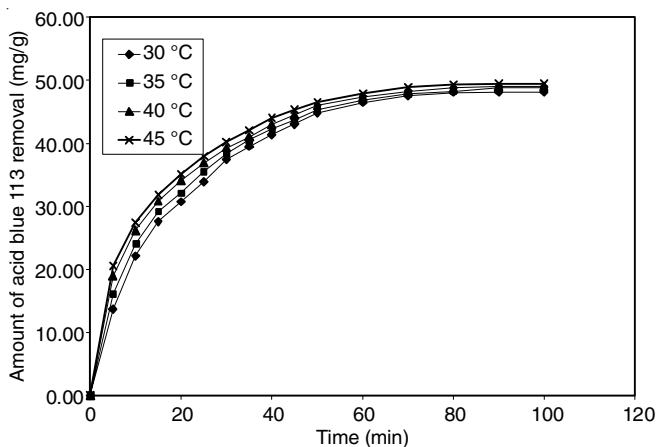


Fig. 4. Amount of acid blue 113 adsorption onto nanocarbon spheres - temperature variation

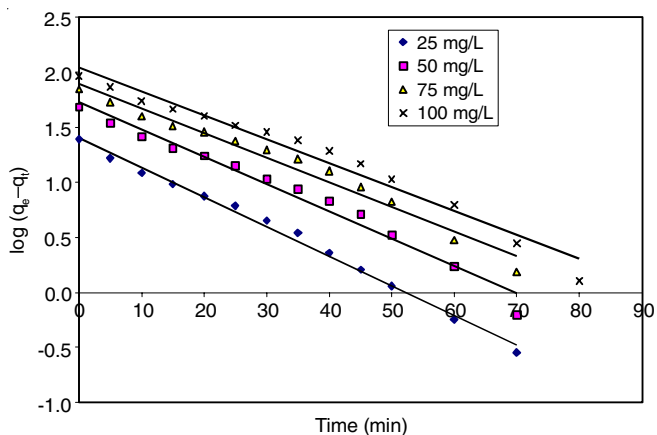


Fig. 5. Pseudo-first order plot for the adsorption of acid blue 113 adsorption onto nanocarbon spheres - concentration variation

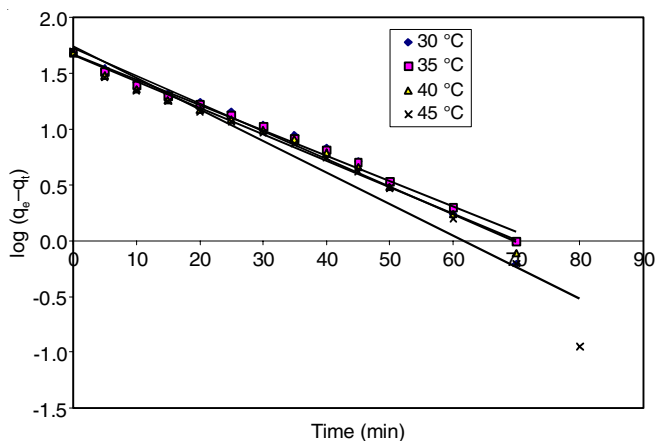


Fig. 6. Pseudo-first order plot for the adsorption of acid blue 113 adsorption onto nanocarbon spheres - temperature variation

pseudo-first order rate constant  $k_1$  decreases from  $6.22 \times 10^{-2}$  to  $4.99 \times 10^{-2} \text{ min}^{-1}$  on increasing the initial acid blue 113 concentration from 25 to 100 mg/L and it varies from  $5.25 \times 10^{-2}$  to  $6.52 \times 10^{-2} \text{ min}^{-1}$  under the range of temperature studied. The  $q_e$  calculated from the pseudo-first order model showed a similarities with respect to the experimental values under various concentrations, but not show any sequential variation with that of experimental values under different temperature range. The correlation coefficient values for the pseudo-first order model

are between 0.9701 to 0.9939 and 0.9496 to 0.9923 under different acid blue 113 concentrations and temperatures, respectively. The adsorption of acid blue 113 by nanocarbon sphere obeys the pseudo-first order criteria for most of the equilibration periods.

**Pseudo-second order kinetic model:** The adsorption of solute onto a solid surface may vary with respect to the variation of any two concentration terms, in such case the adsorption will obey pseudo-second order kinetics. The linear form of pseudo-second order plot for the adsorption of acid blue 113 onto nanocarbon sphere at different concentrations and temperatures are shown in Figs. 7 and 8, respectively. The results derived from the slope and intercept of the pseudo-second order models are calculated.

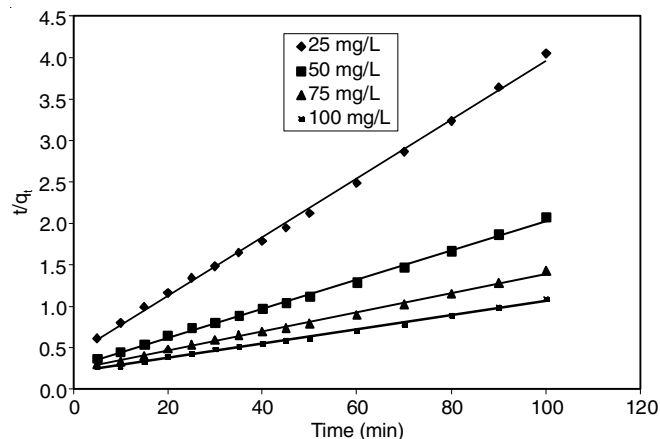


Fig. 7. Pseudo-second order plot for the adsorption of acid blue 113 adsorption onto nanocarbon spheres - concentration variation

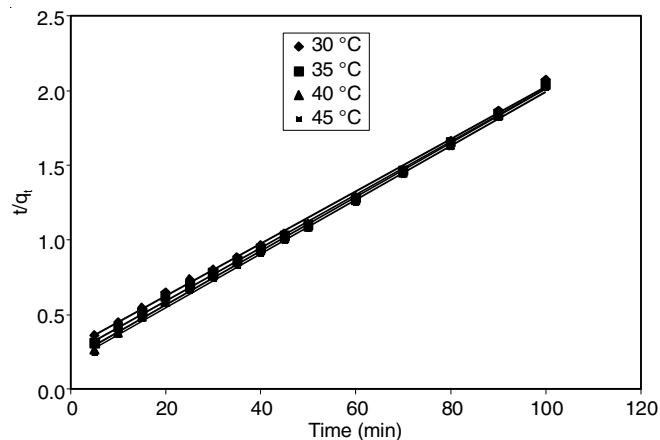


Fig. 8. Pseudo-second order plot for the adsorption of acid blue 113 adsorption onto nanocarbon spheres - temperature variation

The rate constant of pseudo-second kinetic model  $k_2$  decreases from  $2.99 \times 10^{-3}$  to  $0.357 \times 10^{-3} \text{ (g/mg/min)}$  on increasing acid blue 113 concentration from 25 to 100 mg/L. The second order rate constant increases from  $1.121 \times 10^{-3}$  to  $1.77 \times 10^{-3} \text{ (g/mg/min)}$  on increasing the adsorption system temperature from 30 to 45 °C. The  $q_e$ (calcd.) calculated from the pseudo-second order model showed a consistent variation with that of experimental  $q_e$ (exp.) under various initial acid blue 113 concentrations. The  $q_e$ (calcd.) using the pseudo-second order model under different temperatures is not matched with the  $q_e$ (exp.)

values, substantiated the poor applicability of pseudo-second order kinetic model for acid blue 113 adsorption onto nanocarbon sphere.

On analyzing the results of pseudo-first order and pseudo second order kinetic models, the pseudo-first order model is suitable for majority of adsorption periods and pseudo-second order kinetics showed more deviation from the experimental results (Table-2).

**Elovich kinetic model:** The linear form of Elovich plot for the adsorption of acid blue 113 on to nanocarbon sphere is shown in Figs. 9 and 10. The Elovich parameter,  $\alpha$  (mg/g/min) and the initial sorption rate,  $\beta$  (g/mg), the constant related to the energy of activation extent of surface coverage were evaluated from the slope and intercept of linear plots were calculated. On examining the results of Elovich kinetic model, the initial adsorption rate ( $\alpha$ ) decreases from 0.171 to 0.0381 (mg/g/min) and increases from 0.081 to 0.096 (g/mg) on increasing the acid blue 113 concentration and temperature, respectively. The concentration raise reduces the initial sorption rate due to competitive ions, whereas the high temperature favours the initial sorption rate. Another Elovich constant related to energy of activation

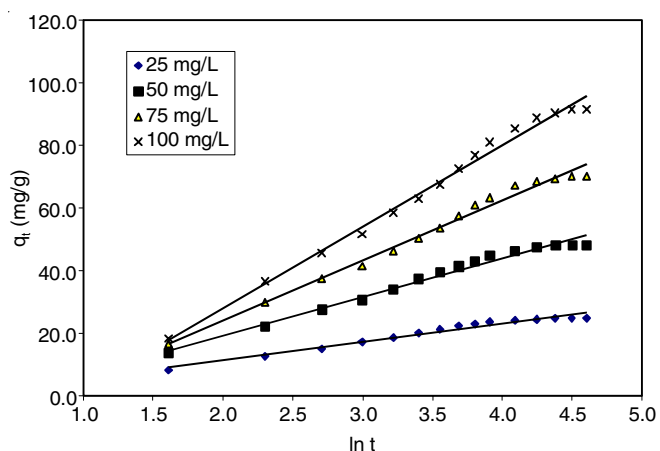


Fig. 9. Elovich plot for the adsorption of acid blue 113 adsorption onto nanocarbon spheres - concentration variation

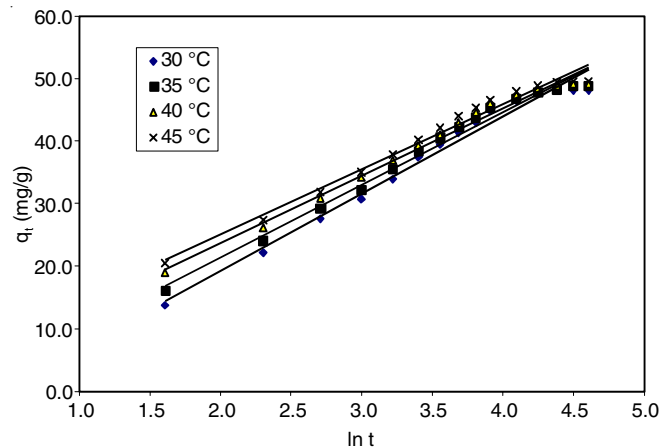


Fig. 10. Elovich plot for the adsorption of acid blue 113 adsorption onto nanocarbon spheres - temperature variation

and extent of surface coverage ( $\beta$ ) increases 5.477 to 10.313 on increasing the initial acid blue 113 concentration and 7.945 to 15.748 on increasing the solution temperature. The  $r^2$  value of Elovich model varied between 0.9667 to 0.9916 and 0.9818 to 0.9841 under different concentrations and temperatures indicate the good degree of fitness of Elovich model for the acid blue 113 adsorption by nanocarbon sphere.

**Intra-particle diffusion model:** The intra-particle diffusion plot for acid blue 113 adsorption into nanocarbon sphere under various concentration and temperatures respectively are shown in Figs. 11 and 12, respectively. The results of intra-particle diffusion plot were calculated. The plot shows multi-linearity with three different phases. This multi-linearity in the plot indicate that there are more than one kinetic stage occurs in the acid blue 113 adsorption by nanocarbon sphere [29]. The diffusion of acid blue 113 from the bulk of the solution towards the sorbent surface, which is also the fastest process among all steps, is indicated by the first linear portion. The second and intermediate portion is the intra-particle diffusion of dye molecules, which is also the rate limiting step. The intermediate velocity in the third phase is caused by the diffusion of acid

TABLE-2  
KINETIC PLOTS FOR THE ADSORPTION OF ACID BLUE 113 ONTO NANOCARBON SPHERES

Parameters	Initial dye concentration (mg/L)				Temperature (°C)			
	25	50	75	100	30	35	40	45
$q_e$ exp. (mg/g)	24.72	48.17	70.04	91.60	48.17	48.78	49.09	49.51
Pseudo first order kinetics								
$k_1$ (min <sup>-1</sup> )	0.0622	0.0571	0.0514	0.0499	0.0571	0.0525	0.0543	0.0652
$q_e$ cal (mg/g)	25.54	53.27	78.34	109.40	53.27	46.96	45.70	55.58
$r^2$	0.9939	0.9763	0.9741	0.9701	0.9763	0.9923	0.9868	0.9496
Pseudo second order kinetics								
$k_2 \times 10^{-3}$ (g/mg/min)	2.990	1.121	0.579	0.357	1.121	1.328	1.598	1.770
h	2.386	3.662	4.303	4.822	3.662	4.193	4.878	5.345
$q_e$ cal (mg/g)	28.25	57.14	86.21	116.28	57.14	56.18	55.25	54.95
$r^2$	0.998	0.9979	0.9968	0.9964	0.9979	0.9988	0.9988	0.9989
Elovich model								
$\alpha$ (mg/g/min)	0.171	0.081	0.052	0.038	0.081	0.086	0.093	0.096
$\beta$ (g/mg)	5.477	7.945	9.165	10.313	7.945	9.865	13.241	15.748
$r^2$	0.9667	0.9818	0.9874	0.9916	0.9818	0.9834	0.9841	0.982
Intra particle diffusion model								
$k_{id}$ (mg/g/min <sup>1/2</sup> )	0.664	2.088	4.003	6.034	2.088	1.879	1.755	1.810
$r^2$	0.9721	0.9932	0.9485	0.9981	0.9932	0.9932	0.9952	0.993

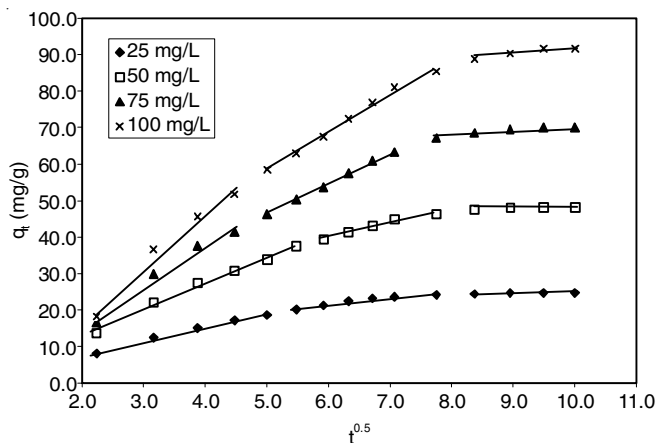


Fig. 11. Intra-particle diffusion plot for the adsorption of acid blue 113 adsorption onto nanocarbon spheres - concentration variation

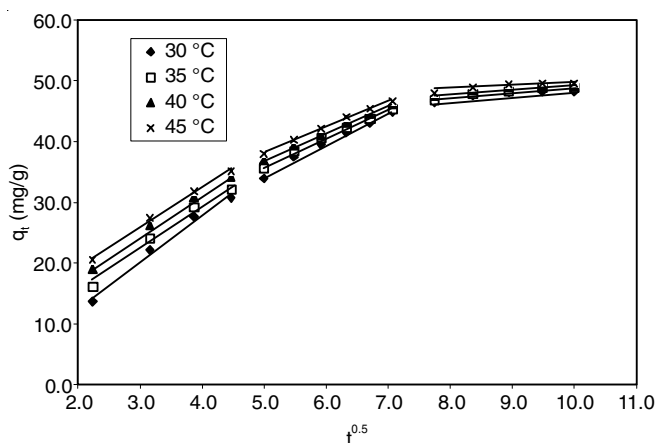


Fig. 12. Intra-particle diffusion plot for the adsorption of acid blue 113 adsorption onto nanocarbon spheres - temperature variation

blue 113 into the interior pores of nanocarbon sphere. After the linear portion, the third portion is the equilibrium stage [29]. The intra-particle diffusion rate constant  $k_{id}$  was evaluated for the second step (as the first step is the fastest and it is not considered for the rate calculation).

As observed from Figs. 11 and 12, the linear portion (second phase) of the plot does not pass through the origin, which is an indication that intra-particle diffusion is not the sole rate limiting step. The final stages are predominantly controlled by intra-particle diffusion and initial stage may be external mass transfer mechanism [30].

**Adsorption isotherm analysis:** For an adsorption system, the evaluation of adsorption isotherm is essential to design and optimization purpose. The isotherm parameters are essential for the evaluation of adsorption probability and adsorption efficiency [31]. Generally, an adsorption isotherm describes the variation of solute adsorption with respect to the change in concentration of solute. At a given temperature, the capacity is directly related to the concentration of solute molecules. Though there are plenty of isotherm models are proposed by various scientists, the fundamental and earliest isotherm models Langmuir and Freundlich isotherm models were used. The isotherm data for acid blue 113 adsorption onto nanocarbon sphere is given in Table-3 by varying the solution temperature from 30 to 45 °C.

TABLE-3  
ISOTHERM STUDY RESULTS OF  
ACID BLUE 113 ADSORPTION

Parameters	Temperature (°C)			
	30	35	40	45
Langmuir isotherm				
$Q_0$ (mg/g)	107.53	104.17	101.52	101.01
$b_L$ (L/mg)	0.6503	0.9143	1.4485	2.2000
$r^2$	0.7917	0.8526	0.9019	0.9343
$R_L$	0.010 to 0.011			
Freundlich isotherm				
$n$	1.55	1.98	3.11	2.47
$k_f$ ( $\text{mg}^{-1/n} \text{L}^{1/n} \text{g}^{-1}$ )	28.70	36.64	47.61	49.95
$r^2$	0.8928	0.7792	0.6056	0.7540

**Langmuir isotherm:** As the isotherm is derived with an assumption of monolayer adsorption, when a sorbent surface site is occupied by a dye molecule, there is no further adsorption on that particular site [32]. Another fact is that when the sorbent surface is homogeneous means all the sites available for the solute is energetically equivalent. When a single layer adsorption is completed, there is no further adsorption occurs.

The Langmuir plot for acid blue 113 adsorption onto nanocarbon sphere is given in Fig. 13 and the results from the slope and intercepts were calculated. The Langmuir monolayer capacity decreases from 107.53 to 101.01 mg/g on increasing the system temperature from 30 to 45 °C. From the kinetic studies, it was proved that adsorption of acid blue 113 by nanocarbon sphere is an endothermic process, but Langmuir monolayer capacity showed a decreasing trend on increasing the temperature. The Langmuir monolayer capacity observed in the present study is comparable with the results reported by the past researchers [30-32]. The dimensionless equilibrium parameter  $R_L$  ranged between 0 to 1.0 indicates the favourability of adsorption under the given set of operating conditions.

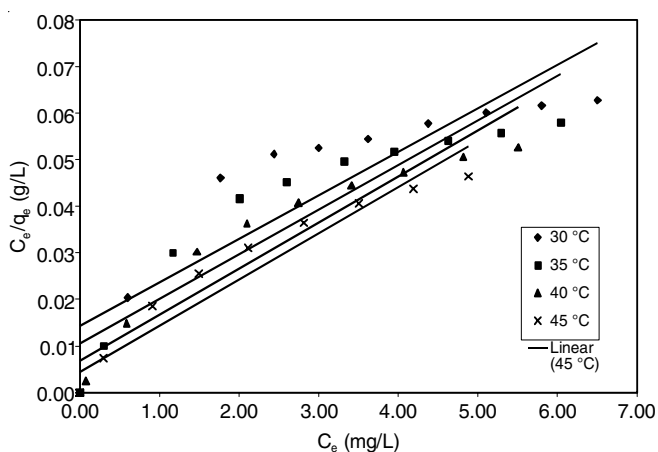


Fig. 13. Langmuir isotherm plot for the acid blue 113 adsorption onto nanocarbon spheres

**Freundlich isotherm:** The linear form of the Freundlich adsorption isotherm plot for the adsorption of acid blue 113 onto nanocarbon sphere is shown in Fig. 14 and the isotherm constants were calculated. The Freundlich constant  $k_f$  related to the quantity of acid blue 113 adsorption for unit equilibrium concentration increased from 28.70 to 49.95 ( $\text{mg L}^{-1/n} \text{L}^{1/n} \text{g}^{-1}$ ) on increasing the solution temperature from 30 to 45 °C. Another

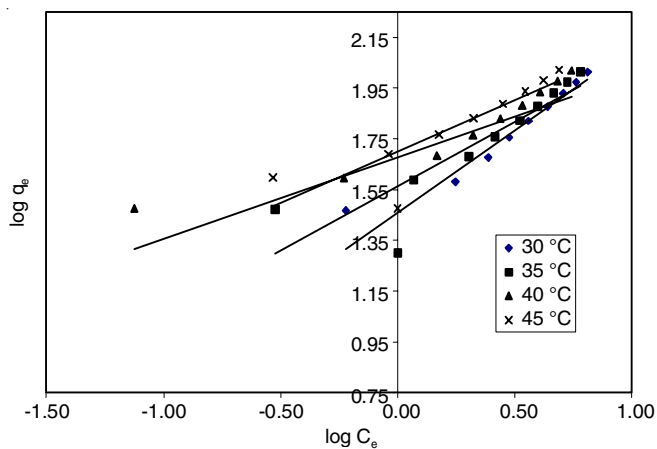


Fig. 14. Freundlich isotherm plot for the acid blue 113 adsorption onto nanocarbon spheres

constant  $1/n$  related to the adsorption intensity of dye onto the adsorption intensity of dye onto the adsorbent or surface heterogeneity. If the value of  $1/n$  is closer to zero (the value of  $n$  between 1 to 10), the adsorption become more and more heterogeneous. As observed from Table-3, the constant  $n$  increased from 1.55 to 2.47, indicating the normal Langmuir type of adsorption involving more surface heterogeneity. On analyzing the correlation coefficient, the  $r^2$  value of Langmuir isotherm is more when compared with Freundlich model, substantiated that the adsorption of acid blue 113 onto nanocarbon sphere follows monolayer adsorption and the surface of nanocarbon sphere is energetically homogeneous.

**Thermodynamics:** Based on the variation of adsorption with respect to temperature, thermodynamic parameters which govern the adsorption were evaluated. The liner plot of  $1/T$  vs.  $\ln K_c$  for the adsorption of acid blue 113 onto nanocarbon sphere is shown in Figs. 15 and the parameters  $\Delta H$  and  $\Delta S$  were evaluated from the slope and the values of intercept of the plot are provided in Table-4.

The negative sign of Gibbs free energy indicated the spontaneous nature of acid blue 113 adsorption onto the surface of nanocarbon sphere. On increasing the temperature, the free energy become more and more negative indicated that the high temperature favours the adsorption with ease when compared to the lower temperature. The positive nature of enthalpy authen-

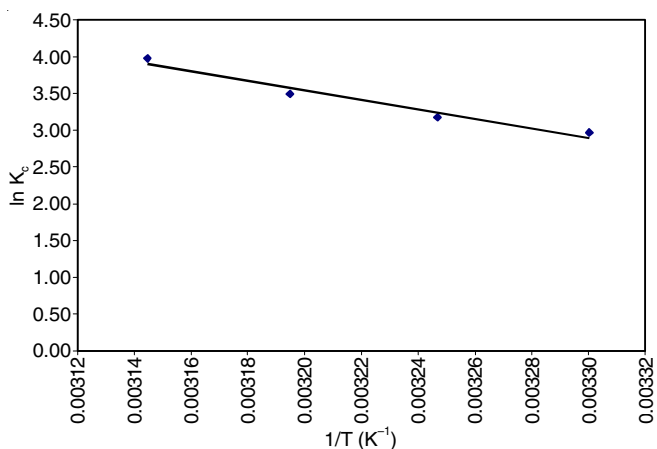


Fig. 15. Thermodynamic plot for the adsorption of acid blue 113 adsorption onto nanocarbon spheres

TABLE-4  
THERMODYNAMIC PARAMETERS FOR ACID BLUE 113  
ADSORPTION ONTO NANOCARBON SPHERES

Temp. (°C)	$\Delta G$ (kJ/mol)	$\Delta H$ (kJ/mol)	$\Delta S$ (J/K/mol)
30	-7.48		
35	-8.13	53.66	201.19
40	-9.10		
45	-10.53		

ticates the endothermic nature of adsorption. The enthalpy values are greater than 40 kJ/mol, indicate that force of attraction between the nanocarbon sphere and acid blue 113 is strong and chemisorptions in nature. The entropy of acid blue 113 adsorption is positive, suggested an increased randomness at the solid and liquid interface [33].

## Conclusion

From the results, it is made clear that the nanocarbon sphere prepared from stems of *Alternanthera sessilis* is an effective adsorbent for the removal of acid blue 113 from its aqueous solution. The adsorption of acid blue 113 is maximum at a pH of 2.0 and it decreases to 86.4 % when the solution pH reaches 12.0. For large scale operations of acid blue 113 adsorption by nanocarbon sphere, the solution must be adjusted to the pH of 10.0. Acid blue 113 dye removal percentage decreased from 98.86 to 91.60 % with an increase of initial acid blue 113 dye concentration from 25 to 100 mg/L. In the present study, adsorption of acid blue 113 dye onto nanocarbon sphere increases from 48.17 to 49.51 mg/g on increasing the temperature from 30 to 45 °C for an initial acid blue 113 dye concentration of 50 mg/L. The increase of adsorption with respect to temperature indicate an endothermic nature, which favoured by increasing temperature. The kinetic study indicates that the pseudo-first order model is suitable for majority of adsorption periods of acid blue 113 and pseudo-second order kinetics showed more deviation from the experimental results. The maximum Langmuir monolayer capacity is found to be 107.53 mg/g at 30 °C. From the thermodynamic studies, it was proved that the adsorption of acid blue 113 by nanocarbon sphere is an endothermic process. The value of Gibbs free energy indicated a spontaneous nature and enthalpy values are greater than 40 kJ/mol indicated that the force of attraction between the nanocarbon sphere and acid blue 113 is strong and chemisorptions in nature.

## CONFLICT OF INTEREST

The authors declare that there is no conflict of interests regarding the publication of this article.

## REFERENCES

1. N. Daneshvar, D. Salari and A.R. Khataee, *J. Photochem. Photobiol. Chem.*, **157**, 111 (2003); [https://doi.org/10.1016/S1016-6030\(03\)00015-7](https://doi.org/10.1016/S1016-6030(03)00015-7).
2. H.R. Javadian, F. Ghorbani, H.A. Tayebi and S.M.H. Asl, *Arab. J. Chem.*, **8**, 837 (2015); <https://doi.org/10.1016/j.arabjc.2013.02.018>.
3. Y. Gan, N. Tian, X. Tian, L. Ma, W. Wang, C. Yang, Z. Zhou and Y. Wang, *J. Porous Mater.*, **22**, 147 (2015); <https://doi.org/10.1007/s10934-014-9881-9>.
4. M. Anbia and S. Salehi, *Dyes Pigments*, **94**, 1 (2012); <https://doi.org/10.1016/j.dyepig.2011.10.016>.

5. G. Crini and P.M. Badot, *Prog. Polym. Sci.*, **33**, 399 (2008); <https://doi.org/10.1016/j.progpolymsci.2007.11.001>.
6. Q. Qin, J. Ma and K. Liu, *J. Hazard. Mater.*, **162**, 133 (2009); <https://doi.org/10.1016/j.jhazmat.2008.05.016>.
7. S. Aoudj, A. Khelifa, N. Drouiche, M. Hecini and H. Hamitouche, *Chem. Eng. Process.: Process Intensif.*, **49**, 1176 (2010); <https://doi.org/10.1016/j.cep.2010.08.019>.
8. G. Ciardelli, L. Corsi and M. Marcucci, *Resour. Conserv. Recycling*, **31**, 189 (2001); [https://doi.org/10.1016/S0921-3449\(00\)00079-3](https://doi.org/10.1016/S0921-3449(00)00079-3).
9. N. Das, R. Vimala and P. Karthika, *Indian J. Biotechnol.*, **7**, 159 (2008).
10. M. Muthukumar and N. Selvakumar, *Dyes Pigments*, **62**, 221 (2004); <https://doi.org/10.1016/j.dyepig.2003.11.002>.
11. L.W. Man, P. Kumar, T.T. Teng and K.L. Wasewar, *Desalination Water Treat.*, **40**, 260 (2012); <https://doi.org/10.1080/19443994.2012.671257>.
12. M. Sala and M.C. Gutiérrez-Bouzán, *Int. J. Photoenergy*, **2012**, 629103 (2012); <https://doi.org/10.1155/2012/629103>.
13. C. Namasiyayam, M. Dinesh Kumar, K. Selvi, R. Ashruffunissa Begum, T. Vanathi and R.T. Yamuna, *Biomass Bioenergy*, **21**, 477 (2001); [https://doi.org/10.1016/S0961-9534\(01\)00052-6](https://doi.org/10.1016/S0961-9534(01)00052-6).
14. B.H. Hameed, A.L. Ahmad and K.N.A. Latiff, *Dyes Pigments*, **75**, 143 (2007); <https://doi.org/10.1016/j.dyepig.2006.05.039>.
15. J.X. Lin, S.L. Zhan, M.H. Fang, X.Q. Qian and H. Yang, *J. Environ. Manage.*, **87**, 193 (2008); <https://doi.org/10.1016/j.jenvman.2007.01.001>.
16. W. Chu, *Water Res.*, **35**, 3147 (2001); [https://doi.org/10.1016/S0043-1354\(01\)00015-X](https://doi.org/10.1016/S0043-1354(01)00015-X).
17. C. Wu, R.L. Tseng and R.S. Juang, *Sep. Purif. Technol.*, **47**, 10 (2005); <https://doi.org/10.1016/j.seppur.2005.03.013>.
18. A.L. Cazetta, A.M.M. Vargas, E.M. Nogami, M.H. Kunita, M.R. Guilherme, A.C. Martins, T.L. Silva, J.C.G. Moraes and V.C. Almeida, *Chem. Eng. J.*, **174**, 117 (2011); <https://doi.org/10.1016/j.cej.2011.08.058>.
19. D. Schimmel, K.C. Fagnani, J.B.O. Santos, M.A.S.D. Barros and E.A. Silva, *Braz. J. Chem. Eng.*, **27**, 289 (2010); <https://doi.org/10.1590/S0104-66322010000200007>.
20. A. Martins and N. Nunes, *J. Chem. Educ.*, **92**, 143 (2015); <https://doi.org/10.1021/ed500055v>.
21. E.I. Unuabonah and A. Taubert, *Appl. Clay Sci.*, **99**, 83 (2014); <https://doi.org/10.1016/j.clay.2014.06.016>.
22. R.F. Gomes, A.C.N. De Azevedo, A.G.B. Pereira, E.C. Muniz, A.R. Fajardo and F.H.A. Rodrigues, *J. Colloid Interface Sci.*, **454**, 200 (2015); <https://doi.org/10.1016/j.jcis.2015.05.026>.
23. B. Murugesan, A. Sivakumar, A. Loganathan and P. Sivakumar, *J. Taiwan Inst. Chem. Eng.*, **71**, 364 (2017); <https://doi.org/10.1016/j.jtice.2016.11.020>.
24. K. Kohse-Höinghaus, J. Troe, J.-U. Grabow, M. Olzmann, G. Friedrichs and K.-D. Hungenbergf, *Phys. Chem. Chem. Phys.*, **20**, 10561 (2018); <https://doi.org/10.1039/C8CP90054J>.
25. Y.H. Magdy and H. Altaher, *J. Environ. Chem. Eng.*, **6**, 834 (2018); <https://doi.org/10.1016/j.jece.2018.01.009>.
26. V. Priya, S.K. Krishna, V. Sivakumar and P. Sivakumar, *Rasayan J. Chem.*, **11**, 1663 (2018); <https://doi.org/10.31788/RJC.2018.1145027>.
27. A.S. Ozcan and A. Ozcan, *J. Colloid Interface Sci.*, **276**, 39 (2004); <https://doi.org/10.1016/j.jcis.2004.03.043>.
28. K.A. Krishnan and T.S. Anirudhan, *Indian J. Chem. Technol.*, **9**, 32 (2002).
29. W.S. Alencar, E.C. Lima, B. Royer, B.D. dos Santos, T. Calvete, E.A. da Silva and C.N. Alves, *Sep. Sci. Technol.*, **47**, 513 (2012); <https://doi.org/10.1080/01496395.2011.616568>.
30. V. Fierro, V. Torné-Fernández, D. Montané and A. Celzard, *Micropor. Mesopor. Mater.*, **111**, 276 (2008); <https://doi.org/10.1016/j.micromeso.2007.08.002>.
31. X. Wang, C. Jiang, B. Hou, Y. Wang, C. Hao and J. Wu, *Chemosphere*, **206**, 587 (2018); <https://doi.org/10.1016/j.chemosphere.2018.04.183>.
32. K. Gul, S. Sohni, M. Waqar, F. Ahmad and N.A. Nik Norulaini and A.K. Mohd. Omar *Carbohydr. Polym.*, **152**, 520 (2016); <https://doi.org/10.1016/j.carbpol.2016.06.045>.
33. M. Goswami and P. Phukan, *J. Environ. Chem. Eng.*, **5**, 3508 (2017); <https://doi.org/10.1016/j.jece.2017.07.016>.